BMC Cancer

RESEARCH

Open Access

Utilizing radiomics and dosiomics with AI for precision prediction of radiation dermatitis in breast cancer patients

Tsair-Fwu Lee[1,2,3], Chu-Ho Chang[1], Chih-Hsuan Chi[1], Yen-Hsien Liu[1], Jen-Chung Shao[1], Yang-Wei Hsieh[1], Pei-Ying Yang[1], Chin-Dar Tseng[1], Chien-Liang Chiu[1], Yu-Chang Hu[4], Yu-Wei Lin[4], Pei-Ju Chao[1*], Shen-Hao Lee[1,5*] and Shyh-An Yeh[1,6,7*]

Abstract

Purpose This study explores integrating clinical features with radiomic and dosiomic characteristics into AI models to enhance the prediction accuracy of radiation dermatitis (RD) in breast cancer patients undergoing volumetric modulated arc therapy (VMAT).

Materials and methods This study involved a retrospective analysis of 120 breast cancer patients treated with VMAT at Kaohsiung Veterans General Hospital from 2018 to 2023. Patient data included CT images, radiation doses, Dose-Volume Histogram (DVH) data, and clinical information. Using a Treatment Planning System (TPS), we segmented CT images into Regions of Interest (ROIs) to extract radiomic and dosiomic features, focusing on intensity, shape, texture, and dose distribution characteristics. Features significantly associated with the development of RD were identified using ANOVA and LASSO regression (p-value < 0.05). These features were then employed to train and evaluate Logistic Regression (LR) and Random Forest (RF) models, using tenfold cross-validation to ensure robust assessment of model efficacy.

Results In this study, 102 out of 120 VMAT-treated breast cancer patients were included in the detailed analysis. Thirty-two percent of these patients developed Grade 2^+ RD. Age and BMI were identified as significant clinical predictors. Through feature selection, we narrowed down the vast pool of radiomic and dosiomic data to 689 features, distributed across 10 feature subsets for model construction. In the LR model, the J subset, comprising DVH, Radiomics, and Dosiomics features, demonstrated the highest predictive performance with an AUC of 0.82. The RF model showed that subset I, which includes clinical, radiomic, and dosiomic features, achieved the best predictive accuracy with an AUC of 0.83. These results emphasize that integrating radiomic and dosiomic features significantly enhances the prediction of Grade 2^+ RD.

Conclusion Integrating clinical, radiomic, and dosiomic characteristics into AI models significantly improves the prediction of Grade 2^+ RD risk in breast cancer patients post-VMAT. The RF model analysis demonstrates

*Correspondence:
Pei-Ju Chao
pjchao99@gmail.com
Shen-Hao Lee
tflee@nkust.edu.tw
Shyh-An Yeh
sayeh@outlook.com
Full list of author information is available at the end of the article

that a comprehensive feature set maximizes predictive efficacy, marking a promising step towards utilizing AI in radiation therapy risk assessment and enhancing patient care outcomes.

Keywords Artificial intelligence, Radiomics, Dosiomics, Radiation dermatitis, Breast cancer

Introduction

This study is dedicated to addressing the predictive challenge of radiation dermatitis (RD), a common side effect encountered by breast cancer patients following radiotherapy. Despite significant advancements in radiation treatment technologies such as volumetric modulated arc therapy (VMAT) and intensity modulated radiation therapy (IMRT) in achieving substantial coverage of the planned target volume (PTV) [1], approximately 90% of patients are likely to experience skin tissue damage caused by radiotherapy, known as RD. The severity of RD is directly correlated with the dose of Radiation Therapy (RT), with about 30% of patients potentially experiencing moderate to severe symptoms. This not only affects the patients' comfort and psychological state but may also lead to interruptions in the treatment plan or result in permanent skin changes [2–4]. Therefore, developing a highly accurate predictive model to forecast and mitigate the occurrence of RD is of great importance for improving the treatment process and enhancing the quality of life for patients.

Early studies have established univariate normal tissue complication probability (NTCP) models from dose-volume histogram (DVH) parameters generated by the treatment planning system (TPS) from PTV and surrounding organs, or multivariate machine learning models that incorporate clinical features such as patients' age, height, weight, tumor size, lymph node status, and surgical and treatment methods for predicting RD in breast cancer patients [5–8]. However, the precision of these methods is limited.

In recent years, Radiomics and Dosiomics have revolutionized cancer diagnosis and complication prediction by offering new analytical pathways. Radiomics can extract morphological, intensity, and texture features from regions of interest (ROI) in non-invasive medical images such as computed tomography (CT), magnetic resonance imaging (MRI), and positron emission tomography (PET) scans, providing insights into the biological characteristics of tissues [9–12]. Dosiomics extends this analysis by examining dose distribution uniformity and spatial variability, offering a deeper understanding compared to traditional DVH methods. This integration significantly enhances the predictive power and credibility of models for RD, crucial for optimizing treatment outcomes [13–15]. The application of Radiomics and Dosiomics in predicting RD is well-established, as evidenced by several studies. One study demonstrated improved prediction accuracy for acute skin toxicity using a dosiomics model in a linear accelerator setup [16], another showed promising results from using a Bayesian-optimized classifier framework on 4D-CT scans for radiodermatitis prediction [17], and a multicenter study emphasized the effectiveness of data encapsulation and dose-gradient radiomics in clinical applications [18]. Collectively, these studies highlight the profound potential of these technologies in enhancing RD prediction accuracy.

The objective of this study is to investigate how to effectively integrate Radiomics and Dosiomics technologies and utilize artificial intelligence (AI) models to improve the prediction accuracy of radiation-induced skin reactions (RD) risk in breast cancer patients following radiotherapy, thereby providing more accurate decision support for clinical physicians.

Materials and methods

Data collection

This study utilized radiomics and dosiomics to evaluate the occurrence of RD in patients treated with VMAT. We examined records from 120 breast cancer patients who completed a standard VMAT protocol of 50Gy over 25 fractions at Kaohsiung Veterans General Hospital from 2018 to 2023. Exclusion criteria included patients who had undergone tumor or breast surgery, received electron beam boost, did not complete the prescribed course of treatment, or had interruptions in their treatment. Clinical and dosimetry data were meticulously collected after treatment, with regions of interest (ROIs) clearly delineated using the Treatment Planning System (TPS; Pinnacle3 versions 9.8 and 14, Philips Radiation Oncology Systems, Fitchburg, WI). All relevant data, including CT images, structural setups, and treatment plans alongside dose distributions, were exported in Digital Imaging and Communications in Medicine (DICOM) format, which encompasses RTDOSE files. These were integral for subsequent data analysis and the development of the RD predictive model. The research framework is outlined in Fig. 1, illustrating the stages of data collection, feature extraction, feature selection, and model development and evaluation. This study received approval from the Institutional Review Board (IRB) at Kaohsiung Veterans General Hospital (KSVGH23-CT12-09), and the need for informed consent was waived due to the retrospective nature of the study.

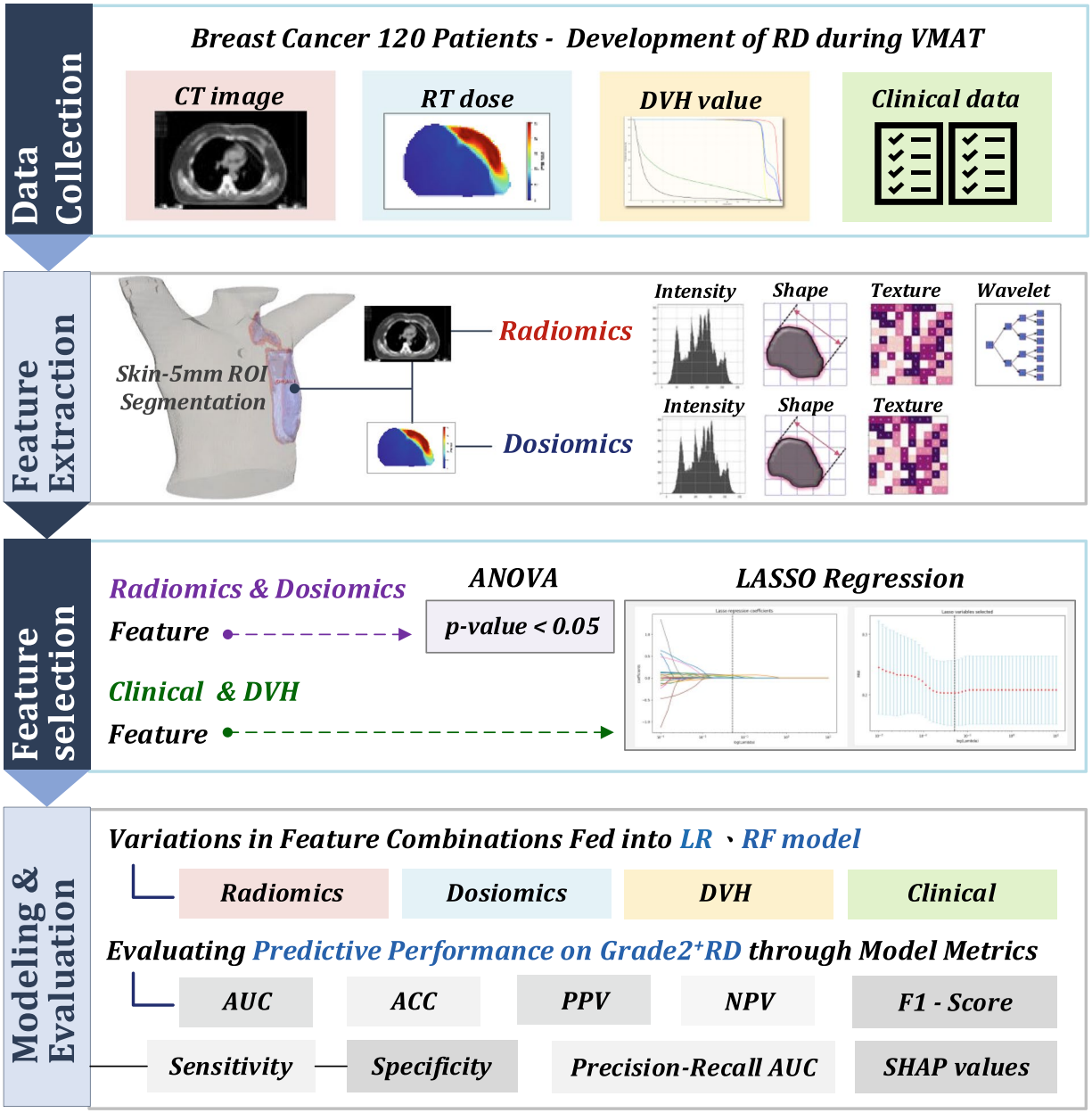

Fig. 1 The flowchart of the study protocol. Abbreviation: VMAT, Volumetric Modulated Arc Therapy; CT, Computed Tomography; RT, Radiation Therapy; DVH, Dose-Volume Histogram; mm, millimeters; ANOVA, Analysis of Variance; LASSO, Least Absolute Shrinkage and Selection Operator; ROI, Region of Interest; RF, Random Forest; RD, Radiation Dermatitis; AUC, Area Under the Receiver Operating Characteristic Curve; NPV, Negative Predictive Value; ACC, Accuracy

Volumetric Modulated Arc Therapy (VMAT) technique

All patients were positioned supinely with arms elevated, scanned using a GE Discovery CT590 RT (GE Healthcare, USA) set to a slice thickness of 2.5 mm and a resolution of 512×512 pixels. Depending on the affected side, either the left or right breast and associated at-risk lymph node regions were targeted. The treatment was delivered using Synergy or Versa HD linear accelerators (Elekta AB, Stockholm, Sweden), with a photon energy of 6 MV. Each patient underwent 25 VMAT sessions, receiving 2Gy per session.

Radiation Dermatitis (RD) assessment

In our study, we conducted a meticulous analysis of retrospective follow-up records from the VMAT treatment period to gather comprehensive clinical data on RD.

We focused specifically on the most severe instances of RD diagnosed in each patient throughout the treatment course, from the onset of therapy. These instances were independently evaluated by expert radiation oncologists using the established Radiation Therapy Oncology Group (RTOG) criteria and systematically recorded in the Hospital Information System (HIS). RD is graded by RTOG as follows: Grade 0 shows no noticeable change from pre-treatment; Grade 1 includes mild symptoms such as faint erythema, hair loss, dry desquamation, and reduced sweating; Grade 2 presents more pronounced reactions like tender erythema or moderate edema; Grade 3 involves severe conditions including widespread moist desquamation outside of skin folds; and Grade 4 includes critical issues such as skin ulceration, spontaneous bleeding, or necrosis.

The primary endpoint of this study was to identify occurrences of moderate to severe RD, classified as Grade 2 or higher, with such cases documented as '1' and less severe reactions as '0'. By focusing on the peak severity of RD observed at any time during treatment, our approach accounts for the maximum impact of radiation on each patient's skin health, providing a comprehensive evaluation of the worst-case scenarios. This method is essential for accurately documenting the peak severity of RD and evaluating the effectiveness of radiation therapy and management strategies in mitigating the most significant adverse effects.

Feature extraction

Clinical and DVH features

We collected clinical data on 120 breast cancer patients from the hospital's Health Information System (HIS). These data included age, gender, Body Mass Index (BMI), cancer stage as defined by the American Joint Committee on Cancer (AJCC), types of surgical intervention, involvement of supraclavicular fossa (SCF) or internal mammary nodes (IMN), and whether chemotherapy was administered, amounting to eight variables in total.

In the TPS, based on CT scans of these patients, twelve Regions of Interest (ROIs) were precisely delineated. These ROIs were marked 5mm beneath the skin on the side affected by breast cancer, for radiation exposure levels from V_{5Gy} up to V_{50Gy} (in 5Gy increments) and specifically for areas receiving 100% ($PTV_{100\%}$) and 105% ($PTV_{105\%}$) of the prescribed dose. The DVH feature parameters from these ROIs were extracted using the TPS. Fig. 2 provides a schematic illustration of the 12 calculated ROIs used in this study.

Radiomics and dosiomics features

As shown in Fig. 2, we employed the PyRadiomics software tool (version 3.1.0, Python 3.9) [19] to conduct quantitative analyses on CT scans with premarked ROIs and available dose distribution data. This process involved extracting a detailed set of image features from the specified ROIs to assess radiomic characteristics comprehensively. The features extracted included: 1) Intensity, which involves statistical

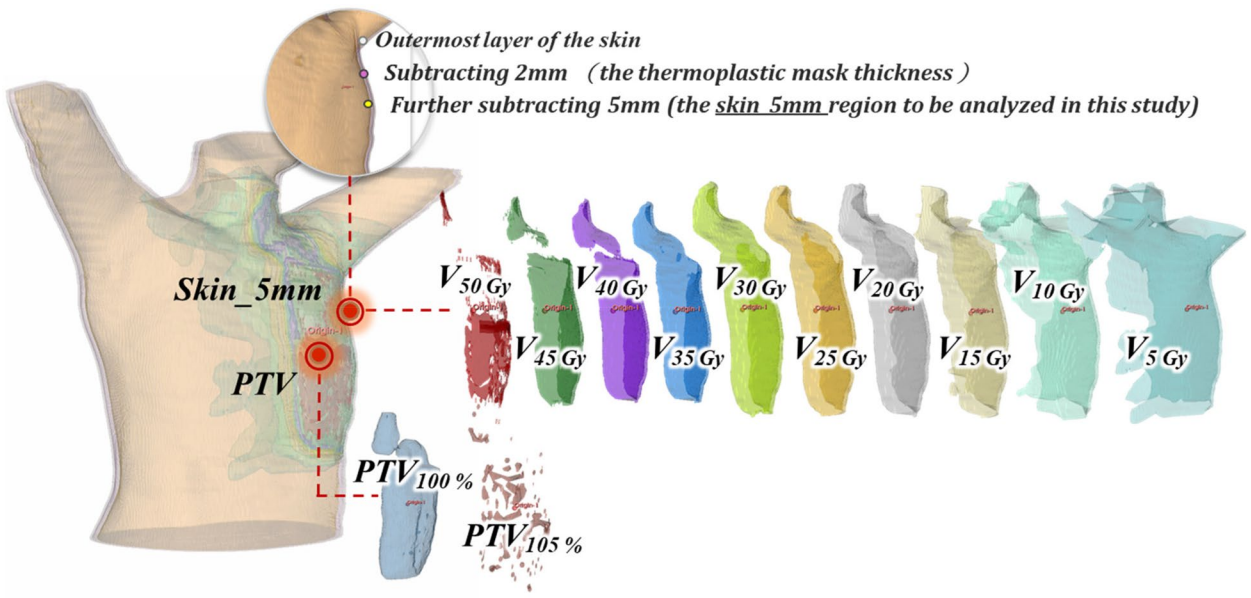

Fig. 2 Schematic illustration of the 12 calculated Regions of Interest (ROIs) in this study. Abbreviation: PTV, Planning Target Volume; V_X Gy, Volume in cubic centimeters of skin receiving x dose of Gray; $PTV_{X\%}$, Planning Target Volume Receiving x % of the Prescription Dose

descriptors like mean, median, and standard deviation that outline the distribution of pixel intensities within the ROIs; 2) Shape, detailing the geometric dimensions such as area, perimeter, and maximum diameter of the ROIs; 3) Texture, analyzing pixel patterns and arrangements using methods like the Gray Level Co-occurrence Matrix (GLCM); and 4) Wavelet, a technique that captures image details across multiple scales and orientations through wavelet transform, enhancing the detection of intricate image details. These features collectively facilitate a robust examination of the radiomic attributes essential for the study.

Dosiomics employed the RTDOSE files exported from the TPS for feature transformation, focusing on extracting dose-related image features. This includes a detailed analysis of dose distribution within the ROI, such as dose uniformity, the location and size of hotspots, and dose-volume related parameters. These metrics are crucial for assessing the quality of radiation treatment plans and predicting treatment outcomes.

In this initial phase, the extraction process yielded 9,996 radiomics features and 1,260 dosiomics features. The outcome of this feature extraction provides the essential quantitative data required for the subsequent steps of feature selection and model development. Fig. 1 offers a visual representation of these features, including histograms, shape outlines, texture patterns, and dose distribution maps, underscoring the diversity and complexity of the information extracted from the original images.

This study adhered to the standards of the Image Biomarker Standardisation Initiative (IBSI) to ensure comparability and standardization across all scans. We maintained uniform voxel sizes for both dose and CT images, with all dose images uniformly collected at 3mm x 3mm x 3mm, and CT images scanned with the same machine, eliminating the need for additional resampling. Image intensities were normalized on a scale from 0 to 100, where 0 represents the minimum and 100 the maximum intensity observed. PyRadiomics supports such normalization, enhancing comparability across different imaging modalities.

For feature extraction, a fixed bin width of 25 Hounsfield Units (HU) was used to quantify gray levels, ensuring the comparability of texture features across various conditions and scans. PyRadiomics also offers adjustable thresholding for ROI segmentation, allowing precise delineation of relevant tissue boundaries. Most parameter settings in PyRadiomics adhere to IBSI guidelines, and while many allow for customization, we predominantly used default settings to maintain consistency throughout our study.

Feature selection and statistical analysis

To differentiate between patients with RD less than Grade 2 and those with Grade 2 or higher (Grade 2^+), chi-square tests were applied to categorical features, while ANOVA was used for continuous features, setting a significance threshold at a p-value of less than 0.05. Features not meeting this criterion were excluded to avoid model overfitting and enhance generalizability. The selected features were then integrated with clinical and DVH parameters to form ten distinct feature subsets for model development.

The LASSO method further refined these subsets by eliminating features not strongly correlated with Grade 2^+ RD. This was achieved through tenfold cross-validation, where LASSO's L1 regularization reduces the coefficients of less significant features to zero. This method effectively manages both continuous and categorical variables and addresses issues of multicollinearity, ensuring that only the most predictive features are retained.

Each subset underwent rigorous testing and validation, enabling the selection of the most appropriate features based on their contribution to the model's predictive accuracy. This comprehensive approach not only enhances understanding of interactions and multicollinearity among variables but also ensures the robustness of the predictive model.

For the final model construction, the refined features were used to train both a RF and a LR model, aimed at predicting the likelihood of patients developing Grade 2^+ RD following VMAT treatment. The entire process, from feature selection using ANOVA and LASSO regression to the precise delineation of features from TPS-exported data, underscores the rigorous methodological framework employed in this study. This approach not only enhances the predictive capability of both models for radiation dermatitis but also provides a reliable methodological foundation for future research, facilitating effective application across various clinical scenarios.

Statistical analysis was conducted using the statistical functions of SciPy (SciPy 1.11.4, Python 3.9), while LASSO regression analysis was implemented using the Scikit-learn package (Scikit-learn 1.3.2, Python 3.9).

Modeling and evaluation of the RD prediction model

In our study, we applied both LR and RF models to assess the risk of RD in patients treated with VMAT for breast cancer. The LR model, renowned for its quick computational ability and ease of use, is ideal for binary outcomes, such as predicting whether a patient will develop Grade 2 or higher RD. This distinguishes it from linear regression models, which are more commonly used for predicting continuous outcomes. Conversely, the RF model excels in handling high-dimensional datasets and avoiding

overfitting, which is essential given the complex mix of clinical, DVH, radiomics, and dosiomics data involved in this research [20–22]. Its resilience to missing data and outliers further solidifies RF's role in enhancing the generalizability of our findings, thereby ensuring that our predictive models are both accurate and robust.

In this research, we meticulously assembled a variety of data elements—radiomics, dosiomics, clinical indicators, and DVH parameters—into ten distinct subsets for analysis. Each subset was carefully crafted through the LASSO regression technique to ensure only the most predictive features were selected for our modeling efforts. Detailed information on the composition and quantity of features within each subset is thoroughly documented in Table S1, located in the supplementary materials. Utilizing these tailored feature sets, we trained the RF model to classify and predict the likelihood of Grade 2^+ RD in patients undergoing breast cancer treatment. To optimize the robustness and accuracy of our models, we implemented a 70:30 split between training and validation datasets, ensuring substantial coverage for model training while reserving enough independent data to accurately evaluate the model's performance. This strategic division supports a detailed assessment and refinement of the model's predictive capabilities, ultimately enhancing its practical application in clinical scenarios.

During the model training phase, tenfold cross-validation was adopted to maximize the generalization ability of the model. This technique splits the entire dataset into 10 equal parts, with each part serving sequentially as the test set and the remaining parts used as the training set. This rotation ensures each data point is used for both training and testing, enhancing the evaluation's accuracy by verifying that the model's performance on new data is consistent with its performance during training.

To address the balance of classification outcomes, we implemented stratified sampling in dividing the data. This approach ensures a consistent ratio of categories within each fold, which is crucial in preventing biases that could arise from imbalanced datasets. By maintaining an even representation of classes across all subsets, our method provides a rigorous and equitable assessment of the model's predictive capabilities, ensuring that the results are dependable and reflective of real-world scenarios.

To evaluate the performance of our predictive model for Grade 2^+ RD in breast cancer patients post-VMAT treatment, we utilized a comprehensive array of metrics: Area Under the Curve (AUC), Positive Predictive Value (PPV), Negative Predictive Value (NPV), Accuracy, F1-Score, and Precision-Recall AUC. These metrics provide a holistic assessment of the model's predictive accuracy and recall capabilities, allowing us to comprehensively gauge its strengths in different scenarios, such as its ability to accurately predict outcomes, manage various error types, and maintain a balance between precision and recall. Additionally, we implemented SHapley Additive exPlanations (SHAP) to interpret the best-performing model, using SHAP values to assess and highlight the most influential features for predicting Grade 2^+ RD in breast cancer patients. This approach not only underscores the model's diagnostic precision but also enriches our understanding of how specific features impact the prediction of RD, thus guiding further enhancements to the model's effectiveness and reliability in clinical settings.

Results

Patient characteristics

We initially collected data on 120 patients. However, following a meticulous screening process which included box plot analysis for outlier detection, 11 patients were excluded from the study. Further exclusions involved 6 patients who had not undergone breast surgery prior to receiving radiation therapy and 1 patient whose V_{50Gy} volume was too small for accurate PyRadiomics calculation. Consequently, the refined cohort comprised 102 patients eligible for final analysis. Within this group, 33 individuals (32%) experienced Grade 2 or higher RD during the treatment period. Detailed clinical characteristics of the participants, including significant correlations between age, BMI, and the incidence of Grade 2^+ RD, are comprehensively tabulated in Table 1. Dosimetry parameters derived from DVH, crucial for assessing radiation exposure, are methodically documented in Table 2. This structured approach ensures a rigorous examination of factors influencing RD, providing a robust dataset for subsequent analyses.

Grade 2^+ RD feature selection

Initially, the patient features assessed included 8 clinical characteristics, 12 DVH parameter features, and 14,364 features each from radiomics and dosiomics. Preliminary screening using ANOVA statistical tests identified 523 radiomics features and 166 dosiomics features. These were further combined with the 8 clinical features and 12 DVH parameter features to create 10 different feature subsets for evaluation. From each feature subset, the LASSO method was employed to identify features highly correlated with Grade 2^+ RD complications to generate the optimal feature combinations. The definition, type of features, number of features, and the top 3 most important features selected by LASSO for each subset combination are listed in Table 3. Detailed features included in each feature subset are provided in Supplementary Table S1.

Table 1 Characteristics of patients with breast cancer treated by VMAT

		during VMAT period		
	Total ***n*** **= 102(100%)**	**with Grade 2$^+$ RD** ***n*** **= 33(32%)**	**< Grade 2** ***n*** **= 69(68%)**	***p*-value**
Age (y)				< 0.05
Mean	57	61	55	
Range	37—81	41 – 81	37 – 77	
BMI				< 0.05
Mean	23.70	24.74	23.20	
Range	16.65 – 32.65	18.05 – 32.65	16.65 – 31.21	
Tumor Laterality				0.784
Left	49 (48%)	17 (17%)	32 (31%)	
Right	53 (52%)	16 (16%)	37 (36%)	
Type of Surgery				0.067
TM	14 (14%)	8 (8%)	6 (6%)	
BCS	88 (86%)	25 (25%)	63 (62%)	
AJCC				0.375
0	26 (25%)	7 (7%)	19 (19%)	
1	36 (35%)	13 (13%)	23 (23%)	
2	29 (28%)	7 (7%)	22 (22%)	
3	8 (8%)	4 (4%)	4 (4%)	
4	3 (4%)	2 (2%)	1 (1%)	
SCF				0.712
No	81 (79%)	25 (25%)	56 (55%)	
Yes	21 (21%)	8 (8%)	13 (13%)	
IMN				0.114
No	87 (85%)	25 (25%)	62 (61%)	
Yes	15 (15%)	8 (8%)	7 (7%)	
Chemotherapy				0.403
No	54 (53%)	15 (15%)	39 (38%)	
Yes	48 (47%)	18 (18%)	30 (29%)	

The grading of dermatitis is defined according to the RTOG grading criteria

For continuous numerical features, the ANOVA test is employed, while for categorical features, the Chi-square test is utilized

VMAT Volumetric modulated arc therapy, *AJCC* American Joint Committee on Cancer, *SCF* Supraclavicular Fossa, *IMN* Internal Mammary Nodes, *ANOVA* Analysis of Variance

Grade 2$^+$ RD prediction model evaluation and feature importance

In this study, the 10 feature subsets detailed in Table 3, each filtered through the LASSO method, were independently evaluated using the LR model. The performance metrics for each subset were presented in Fig. 3(a), with Subset J (comprising DVH, Radiomics, and Dosiomics features) demonstrating the best performance for predicting Grade 2$^+$ RD, achieving an average AUC of 0.82 (represented by a red line). The next best performing subset was Subset I (comprising Clinical, Radiomics, and Dosiomics features), with an average AUC of 0.77.

Additional performance metrics such as Accuracy (ACC), Positive Predictive Value (PPV), Negative Predictive Value (NPV), F1-score, Specificity, and Precision-Recall AUC were tabulated in Table 4. The ACC of the LR model ranged between 0.67 to 0.74, with the highest accuracy observed in subsets containing Clinical, Radiomics, and Dosiomics features—particularly in Subsets I and J. The highest PPV was 0.62, and NPV values consistently exceeded 0.70, indicating the model's stability in predicting both positive and negative instances of Grade 2$^+$ RD. The F1-score varied between 0.36 to 0.60, indicating performance variability across different feature subsets, with Subset J performing optimally.

The Specificity values in the LR model were notably high across all models, demonstrating the model's effectiveness in identifying patients without RD. The Precision-Recall AUC ranged from 0.42 to 0.72, with Subset I achieving the highest score, indicating an optimal balance between precision and recall.

Table 2 Candidate Dose Factors for Breast Cancer Patients Undergoing VMAT

			during VMAT period			
	Total ***n*** **= 102 (100%)**		**with Grade 2$^+$ RD** ***n*** **= 33 (32%)**		**< Grade 2** ***n*** **= 69 (68%)**	
Feature	**Range (cc)**	**Mean ± SD (cc)**	**Range (cc)**	**Mean ± SD (cc)**	**Range (cc)**	**Mean ± SD (cc)**
V_5	151.85—689.46	296.77 ± 106.84	151.85—576.46	328.20 ± 113.12	166.27—689.46	281.74 ± 101.11
V_{10}	131.52—495.88	235.11 ± 75.98	131.52—465.14	259.28 ± 82.90	137.90—495.88	223.54 ± 70.16
V_{15}	120.33—388.06	206.67 ± 59.67	120.33—353.85	226.84 ± 65.35	122.99—388.06	197.03 ± 54.64
V_{20}	112.44—328.19	187.99 ± 49.42	112.44—302.90	205.13 ± 54.99	114.71—328.19	179.79 ± 44.65
V_{25}	105.52—274.05	172.69 ± 41.26	105.52—274.05	188.33 ± 46.76	108.11—271.75	165.21 ± 36.39
V_{30}	99.47—243.86	159.13 ± 35.20	99.47—243.86	172.07 ± 39.67	101.19—228.71	152.94 ± 31.30
V_{35}	92.86—213.55	146.09 ± 30.42	93.52—213.55	156.76 ± 33.14	92.86—201.92	140.99 ± 27.86
V_{40}	82.37—192.09	132.34 ± 27.11	86.71—192.09	141.37 ± 28.32	82.37—182.12	128.03 ± 25.61
V_{45}	63.50—159.48	110.57 ± 23.22	74.49—159.48	118.35 ± 23.85	63.50—149.97	106.85 ± 22.13
V_{50}	13.31—107.64	42.05 ± 18.07	13.31—107.64	45.61 ± 22.17	13.59—81.78	40.35 ± 15.64
$PTV_{100\%}$	187.65 -1599.94	619.98 ± 289.09	187.65—1599.94	737.73 ± 348.59	199.56—1346.79	563.66 ± 238.74
$PTV_{105\%}$	0.15—461.17	45.93 ± 67.69	0.39—300.11	61.79 ± 75.67	0.15—461.17	38.35 ± 62.70

VMAT Volumetric modulated arc therapy, *mm* millimeters, *cc* cubic centimeters, *SD* Standard Deviation, V_{X_Gy} Volume in cubic centimeters of skin receiving x dose of Gray, $PTV_{X\%}$ Planning Target Volume Receiving x % of the Prescription Dose

The results from the LR model highlight the benefit of combining clinical features with imaging features from Radiomics and Dosiomics. In particular, Subset I (comprising Clinical, Radiomics, and Dosiomics features) showed promising performance.

The RF model's training and testing outcomes for predicting Grade 2$^+$ RD complications in breast cancer patients are presented in Fig. 3(b), where the AUC values for each feature subset are displayed. Subset I (including Clinical, Radiomics, and Dosiomics features) emerged as the most effective model for predicting Grade 2$^+$ RD, with an AUC of 0.83 (represented by a red line). Table 5 lists other performance metrics for the RF model.

The ACC for the RF model ranged from 0.64 to 0.78, with the highest observed in Subset F, which included Radiomics and Dosiomics features. Models built with all feature subsets maintained commendable levels of PPV and NPV, ensuring precise predictions of Grade 2$^+$ RD occurrences. The F1-score ranged from 0.32 to 0.54, demonstrating variability across different combinations of features. Specificity values varied between 0.76 to 0.89, confirming the RF model's effectiveness in identifying patients without RD. The Precision-Recall AUC values ranged from 0.48 to 0.66, with Subset J achieving the highest, indicating the best balance between precision and recall.

The impact of feature combinations on prediction performance is evident, particularly when Radiomics and Dosiomics features are included in both LR and RF models. A comprehensive comparison of the two models indicates that the inclusion of clinical features in Feature Subset I (comprising Clinical, Radiomics, and Dosiomics features) significantly enhances the prediction accuracy and reliability for Grade 2$^+$ RD. This subset consists of 1 clinical feature, 21 Radiomics features, and 5 Dosiomics features. The correlation between features in Subset I and Grade 2$^+$ RD is detailed in Fig. 4, where the LASSO feature importance graph shows blue indicating positive correlations and red indicating negative correlations. This visualization not only underscores the predictive strength of these features but also highlights their specific influence on the outcome.

Figures 5 and 6 illustrate the differences in feature importance between the LR and RF models as depicted by SHAP values, which quantify each feature's impact on the models' ability to predict Grade 2$^+$ RD after training. The color gradient from blue to red indicates the magnitude of the feature values. Higher SHAP values signify a significant impact on predicting Grade 2$^+$ RD, while lower values suggest a lesser impact.

Discussion

Currently, there are relatively few studies utilizing Radiomics and Dosiomics methods for predicting RD responses in breast cancer patients based on CT images. Therefore, this research aims to delve deeper into the potential of Radiomics and Dosiomics approaches for predicting more severe RD responses in breast cancer patients through the analysis of predictive model results from 10 different feature subsets. This exploration seeks to understand whether these methods can offer broader

Table 3 LASSO-Identified Prognostic Feature Correlations in 10 Subsets

Subsets ID	Feature Composition	Feature Count	Top 3 Features in the subset
A	Clinical DVH	4	DVH_PTV$_{100\%}$ Age DVH_V$_{50Gy}$
B	Clinical Radiomics	31	Radiomics_V$_{50Gy}$_wavelet_HLL_glcm_InverseVariance Radiomics_V$_{50Gy}$_wavelet_HLH_firstorder_Mean Radiomics_PTV$_{105\%}$_wavelet_LHL_glcm_InverseVariance
C	Clinical Dosiomics	8	Dosiomics_PTV$_{100\%}$_original_glcm_Idmn Dosiomics_V$_{45Gy}$_original_glszm_LowGrayLevelZoneEmphasis Age
D	DVH Radiomics	32	Radiomics_V$_{50Gy}$_wavelet_HLL_glcm_InverseVariance Radiomics_PTV$_{100\%}$_wavelet_HLL_firstorder_Skewness Radiomics_V$_{50Gy}$_wavelet_HLH_firstorder_Mean
E	DVH Dosiomics	9	Dosiomics_V$_{45Gy}$_original_glszm_LowGrayLevelZoneEmphasis DVH_V$_{50Gy}$ Dosiomics_PTV$_{100\%}$_original_glcm_Idmn
F	Radiomics Dosiomics	36	Radiomics_V$_{50Gy}$_wavelet_HLL_glcm_InverseVariance Dosiomics_PTV$_{100\%}$_original_glrlm_HighGrayLevelRunEmphasis Radiomics_V$_{50Gy}$_wavelet_HLH_firstorder_Mean
G	Clinical DVH Radiomics	32	Radiomics_V$_{50Gy}$_wavelet_HLL_glcm_InverseVariance Radiomics_V$_{50Gy}$_wavelet_HLH_firstorder_Mean Radiomics_PTV$_{105\%}$_wavelet_LHL_glcm_InverseVariance
H	Clinical DVH Dosiomics	11	Dosiomics_V$_{45Gy}$_original_glszm_LowGrayLevelZoneEmphasis DVH_V$_{50Gy}$ Age
I	Clinical Radiomics Dosiomics	27	Radiomics_V$_{50Gy}$_wavelet_HLL_glcm_InverseVariance Dosiomics_PTV$_{100\%}$_original_glrlm_HighGrayLevelRunEmphasis Radiomics_PTV$_{105\%}$_wavelet_LHL_glcm_InverseVariance
J	DVH Radiomics Dosiomics	41	DVH_V$_{50Gy}$ Radiomics_V$_{50Gy}$_wavelet_HLL_glcm_InverseVariance Radiomics_V$_{50Gy}$_wavelet_HLH_firstorder_Mean

LASSO Least Absolute Shrinkage and Selection Operator, *ID* Identifier, *DVH* Dose-Volume Histogram, V_{X_Gy} Volume in cubic centimeters of skin receiving x dose of Gray, $PTV_{X\%}$ Planning Target Volume Receiving x % of the Prescription Dose, *H* High-pass filter, *L* Low-pass filter, *GLCM* Gray Level Co-occurrence Matrix, *GLRLM* Gray Level Run Length Matrix, *GLSZM* Gray Level Size Zone Matrix

assessments and contributions towards forecasting the severity of RD reactions in such patients.

From the AUC metrics presented in Fig. 3(b), the RF model's performance metrics underscore its robustness in predicting Grade 2^+ RD. The best-performing feature subset I, which includes Clinical, Radiomics, and Dosiomics features, achieved an AUC of 0.83, closely followed by subset F, consisting solely of Radiomics and Dosiomics features, with an AUC of 0.81. These results highlight the significant contribution of Radiomics and Dosiomics features in enhancing the prediction of Grade 2^+ RD in breast cancer patients. Comparatively, the RF model generally exhibited higher average accuracy and PPV than the LR model across all feature subsets, indicating a potential overall performance advantage in predicting Grade 2^+ RD. Notably, in the Precision-Recall AUC metric, the LR model's Subset I and the RF model's Subset J performed exceptionally well, achieving an optimal balance between precision and recall.

Given the RF model's superior performance across most metrics, it is recommended for predicting Grade 2^+ RD in breast cancer patients. This recommendation is further supported by the findings of Feng et al. [18], who reported that models using clinical and dosimetry parameters alone, Radiomics features alone, and a combination of all three resulted in validation set AUCs of 0.816, 0.907, and 0.911, respectively. These figures corroborate the substantial role of Radiomics features in boosting the predictive accuracy for Grade 2^+ RD, demonstrating the effectiveness of integrating these advanced imaging and dosimetry analyses for more accurate and reliable RD risk assessments.

Although the AUC of feature subset G (comprising Clinical, DVH parameter, and Radiomics features) achieved 0.78 in LR and 0.72 in RF models in this study, which is lower compared to the AUC of 0.911 for a similar feature combination reported by Feng et al. [18], this discrepancy can be attributed to several factors.

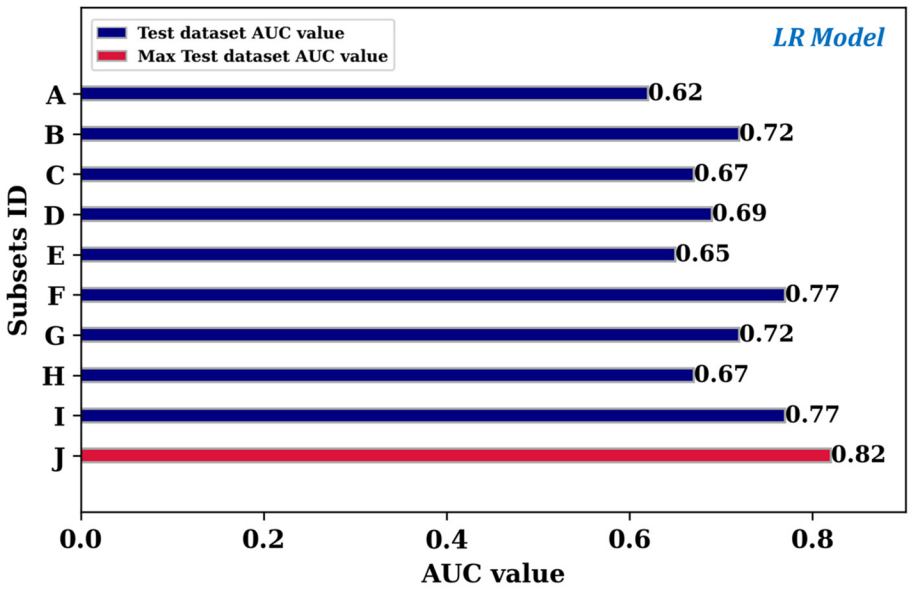

(a)

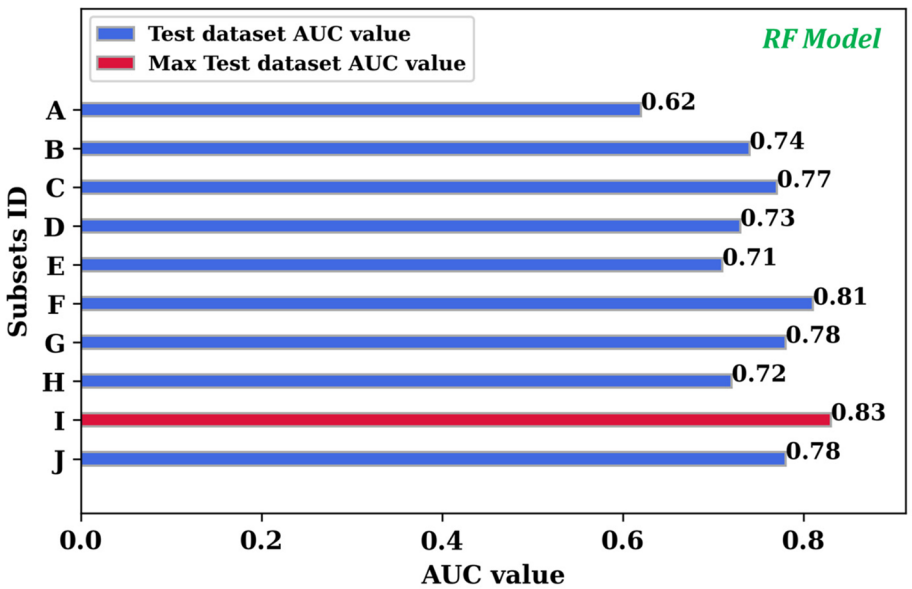

(b)

Fig. 3 AUC Results for ten subsets in Predicting Grade 2^{+} RD: (a) LR Model; (b) RF Model. Abbreviation: ID, Identifier; Val, Validation dataset; LR, Logistic Regression; RF, Random Forest; RD, Radiation Dermatitis; AUC, Area under the receiver operating characteristic curve

Differences in sample sizes, definitions of RD timing, feature selection and ROI planning, data preprocessing, algorithms, hyperparameter settings, patient characteristics, and sample proportions are among the various details that may lead to these variances [17]. Such differences underscore the complexity of modeling and the impact of methodological variations on the performance of predictive models.

RD is a non-stochastic effect where the severity can increase proportionally with the magnitude of the dose received. This notion is supported by studies from Xie et al. [23] and Vicini et al. [24], which highlighted that

Table 4 Prediction of Grade 2^+ radiation dermatitis in breast cancer patients—average performance metrics of the logistic regression model across 10 iterations

Subsets ID	Feature Composition	ACC	PPV	NPV	F1-score	Specificity	Precision-Recall AUC
A	Clinical DVH	0.67	0.53	0.72	0.36	0.81	0.42
B	Clinical Radiomics	0.73	0.62	0.78	0.55	0.94	0.61
C	Clinical Dosiomics	0.72	0.61	0.74	0.45	0.90	0.66
D	DVH Radiomics	0.69	0.53	0.80	0.52	0.93	0.57
E	DVH Dosiomics	0.72	0.59	0.75	0.46	0.88	0.57
F	Radiomics Dosiomics	0.72	0.60	0.78	0.52	0.96	0.70
G	Clinical DVH Radiomics	0.70	0.55	0.78	0.52	0.93	0.62
H	Clinical DVH Dosiomics	0.71	0.62	0.75	0.44	0.87	0.57
I	Clinical Radiomics Dosiomics	0.74	0.59	0.80	0.56	0.93	0.72
J	DVH Radiomics Dosiomics	0.74	0.62	0.82	0.60	0.94	0.67

ID Identifier, *RD* Radiation Dermatitis, *AUC* Area under the receiver operating characteristic curve, *ACC* Accuracy, *PPV* Positive Predictive Value, *NPV* Negative Predictive Value

breast volume significantly influences the incidence of RD following RT in breast cancer patients. Correspondingly, in this study, the LASSO results for the optimal feature subset I, as depicted in Fig. 4, predominantly selected features from the Radiomics and Dosiomics categories that focus on skin areas receiving 100% and 105% of the prescribed dose ($PTV_{100\%}$ and $PTV_{105\%}$). This alignment of findings emphasizes the critical role of dose intensity and affected volume in the development of RD.

The LASSO method was utilized to filter out Radiomics and Dosiomics features significantly correlated with the prediction of Grade 2^+ radiation dermatitis (RD) in breast cancer patients. The selected multidimensional features include texture, shape, and first-order statistical features. According to the results depicted in Fig. 4, Radiomics features, predominantly those transformed by wavelet filters (20 features), were selected due to their potential association with cellular damage, vascular changes, or other structural alterations within the region [25]. Wavelet-filter transformations in our study enhance feature extraction by capturing information at multiple resolutions, which is crucial for identifying texture features. These features, indicative of subtle underlying tissue changes, are revealed through variations in high-frequency and low-frequency signals across different scales and orientations. High-frequency details may correspond to fine structural changes like cellular damage or minor vascular alterations, while low-frequency content often reflects broader anatomical features such as blood vessels [26].

The utility of wavelet-transformed features is particularly noted in their ability to detect changes at the lesion margins from high-frequency signals in the images. This capacity for capturing fine details associated with structural changes in tissues suggests potential pathological alterations, making wavelet transformations valuable in medical image analysis for distinguishing various physiological and pathological conditions [26]. However, it's crucial to recognize that the assumption that these features directly represent specific tissue changes remains

Table 5 Prediction of Grade 2^+ radiation dermatitis in breast cancer patients—average performance metrics of the random forest model across 10 iterations

Subsets ID	Feature Composition	ACC	PPV	NPV	F1-score	Specificity	Precision-Recall AUC
A	Clinical DVH	0.64	0.42	0.70	0.32	0.86	0.48
B	Clinical Radiomics	0.71	0.58	0.73	0.35	0.82	0.59
C	Clinical Dosiomics	0.73	0.64	0.75	0.45	0.89	0.56
D	DVH Radiomics	0.70	0.72	0.72	0.33	0.76	0.54
E	DVH Dosiomics	0.70	0.62	0.74	0.41	0.87	0.59
F	Radiomics Dosiomics	0.78	0.85	0.78	0.54	0.83	0.65
G	Clinical DVH Radiomics	0.73	0.73	0.74	0.43	0.80	0.60
H	Clinical DVH Dosiomics	0.71	0.63	0.74	0.45	0.88	0.57
I	Clinical Radiomics Dosiomics	0.77	0.79	0.77	0.54	0.83	0.59
J	DVH Radiomics Dosiomics	0.76	0.75	0.77	0.50	0.81	0.66

ID Identifier, *RD* Radiation Dermatitis, *AUC* Area under the receiver operating characteristic curve, *ACC* Accuracy, *PPV* Positive Predictive Value, *NPV* Negative Predictive Value

theoretical. We have not yet empirically validated a direct correlation between wavelet-transformed features and specific tissue alterations like cell damage or vascular changes. Consequently, interpretations should be made with caution. Future research should focus on linking these radiomic features with histopathological findings and clinical outcomes to confirm their predictive effectiveness for radiation dermatitis, ensuring the scientific integrity of our findings and guiding clinical applications.

The Radiomics features most highly correlated with Grade 2^+ RD were identified as Radiomics_skin5mm_v45_wavelet-HLL_glcm_InverseVariance and Radiomics_ptv_105_wavelet-LHL_glcm_InverseVariance, where the glcm_InverseVariance feature evaluates the consistency of grayscale values within the image region. This observation suggests that uniform tissue texture in the skin regions of breast cancer patients may reduce their susceptibility to developing moderate to severe RD. While direct evidence linking consistent tissue texture to lower RD incidence is sparse, this concept aligns with findings from Feng H's study [18]. The study indicates that repositioning PTV and skin regions to areas with a lower prevalence of radiomic features associated with moderate to severe RD could potentially lessen the occurrence of these conditions [18]. This supports the hypothesis that homogeneous radiomic characteristics across these regions might positively impact RD outcomes.

Regarding the selected Dosiomics features, since this study did not enhance images with filters before extracting Dosiomics features, the original dose-related features were selected. Dosiomics_ptv_100_original_glszm_SizeZoneNonUniformity reflects the non-uniformity of the radiation dose distribution in the PTV100% area based on dose texture, which may lead to localized tissue receiving higher than expected radiation doses, increasing the risk of Grade 2^+ RD. The feature Dosiomics_ptv_100_original_glrlm_HighGrayLevelRunEmphasis might also indicate that areas of the skin exposed to higher doses are associated with an increased risk of Grade 2^+ RD.

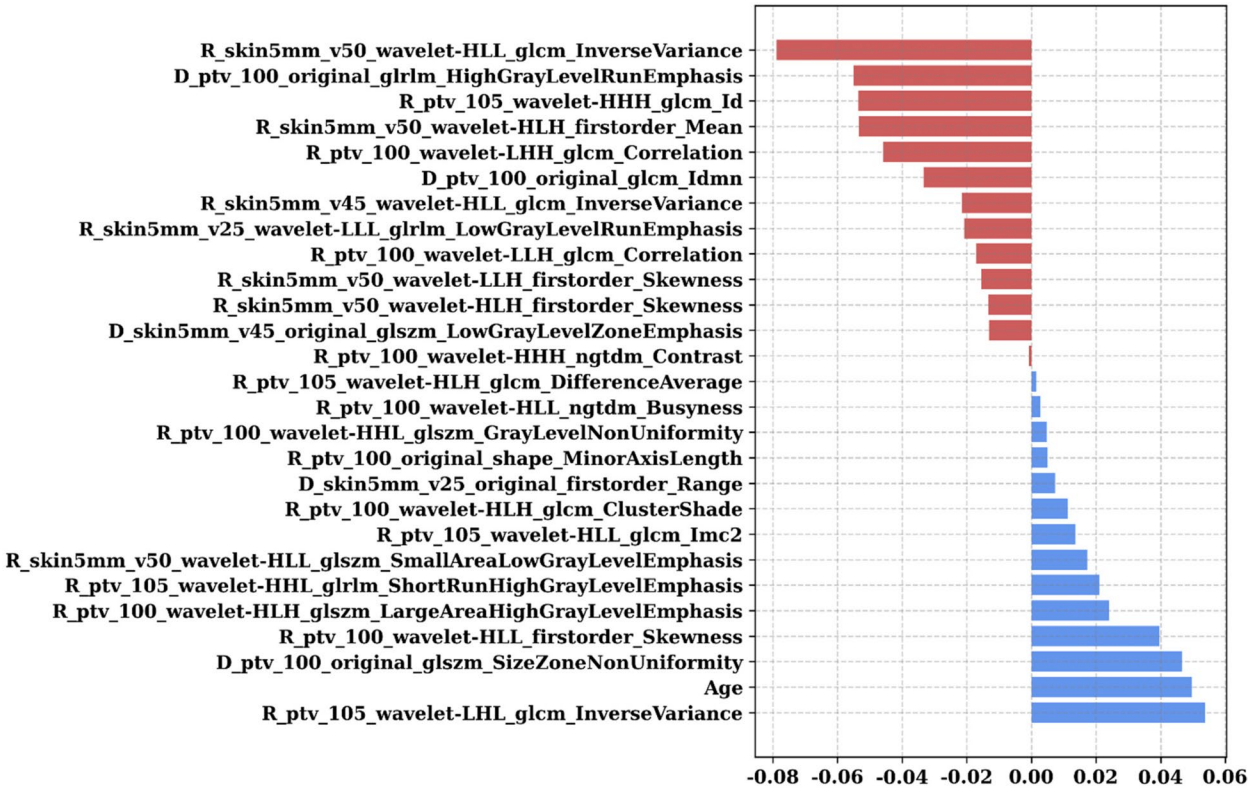

Fig. 4 Feature importance for feature subset I in relation to Grade 2^+ RD, based on LASSO, with blue indicating positive correlation and red indicating negative correlation. Abbreviation: LASSO, Least Absolute Shrinkage and Selection Operator; R, Radiomics; D, Dosiomics; PTV, Planning Target Volume; H, High-pass filter; L, Low-pass filter; GLCM, Gray Level Co-occurrence Matrix; GLRLM, Gray Level Run Length Matrix; GLSZM, Gray Level Size Zone Matrix; RD, Radiation Dermatitis

This result suggests that besides dose levels, the uniformity and texture consistency of skin tissue are crucial factors affecting the occurrence of RD, which can vary among patients. In this study, we derived Dosiomics features and DVH parameters from RT-DOSE files exported from the TPS, utilizing these data to assess the impact of radiation exposure relevant to our analysis of RD.

In this study, the performance of the various feature subsets, as shown in the model results of Fig. 2, indicates that the least effective feature subset A, which has been a common combination in many previous studies on predicting complications, achieved an AUC of only 0.62 in this study. Subset A is composed of clinical information of breast cancer patients and DVH dose parameters calculated by TPS. This may be precisely because the skin dose calculated by TPS is not accurate, preventing the model from learning to predict whether a patient will develop Grade 2^+ RD based on the dose information received by the skin accurately. However, the model results of subsets incorporating Radiomics and Dosiomics features, such as subset D (AUC = 0.73), subset E (AUC = 0.71), subset G (AUC = 0.78), and subset H (AUC = 0.72), demonstrate that combining DVH parameter features with Radiomics and Dosiomics features can effectively enhance the prediction of Grade 2^+ RD in breast cancer patients. Among these, subsets D and G, which incorporate Radiomics features, compared to subsets E and H that include Dosiomics features, further highlight Radiomics' superior assistance in prediction. Overall, these findings may have significant implications for improving radiation treatment planning and reducing the incidence of RD.

The multivariate analysis of the clinical characteristics of the 102 breast cancer patients included in this study and their relationship with RD, as shown in Table 1 and Fig. 4, indicates that laterality, type of surgery, AJCC cancer staging, SCF, IMN, and whether chemotherapy was received are not significantly related to the occurrence of Grade 2^+ RD in this study.

Numerous studies have observed a correlation between higher BMI values and the incidence of more severe RD [6, 27–29], consistent with the results of the ANOVA statistical test (p-value < 0.05) in this study. However, no significant correlation was observed during the LASSO feature importance analysis. This discrepancy may be attributed to the average BMI values of both groups in this study's sample not exceeding 25

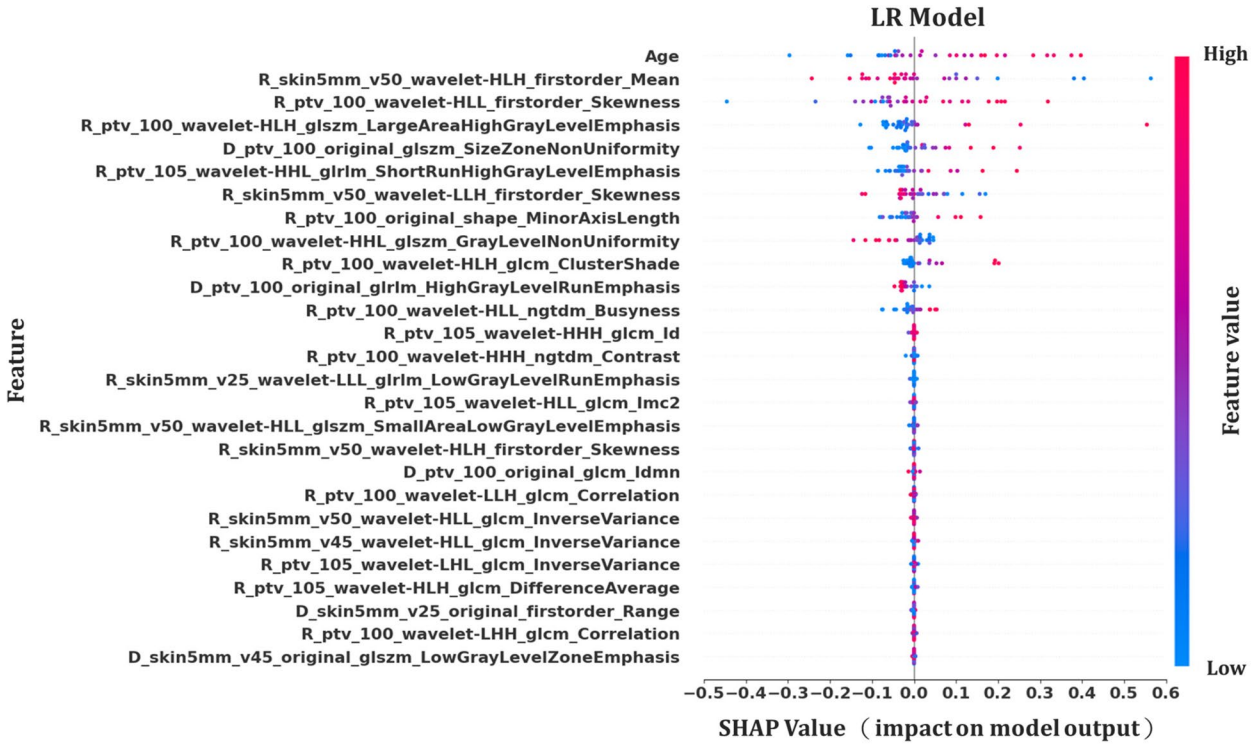

Fig. 5 Bee Swarm Plot of Feature Importance via SHAP Values in the LR Model for Predicting Grade 2^+ RD. Abbreviation: RF, Random Forests; R, Radiomicd; D, Dosiomics; RD, Radiation Dermatitis; SHAP, SHapley Additive exPlanations

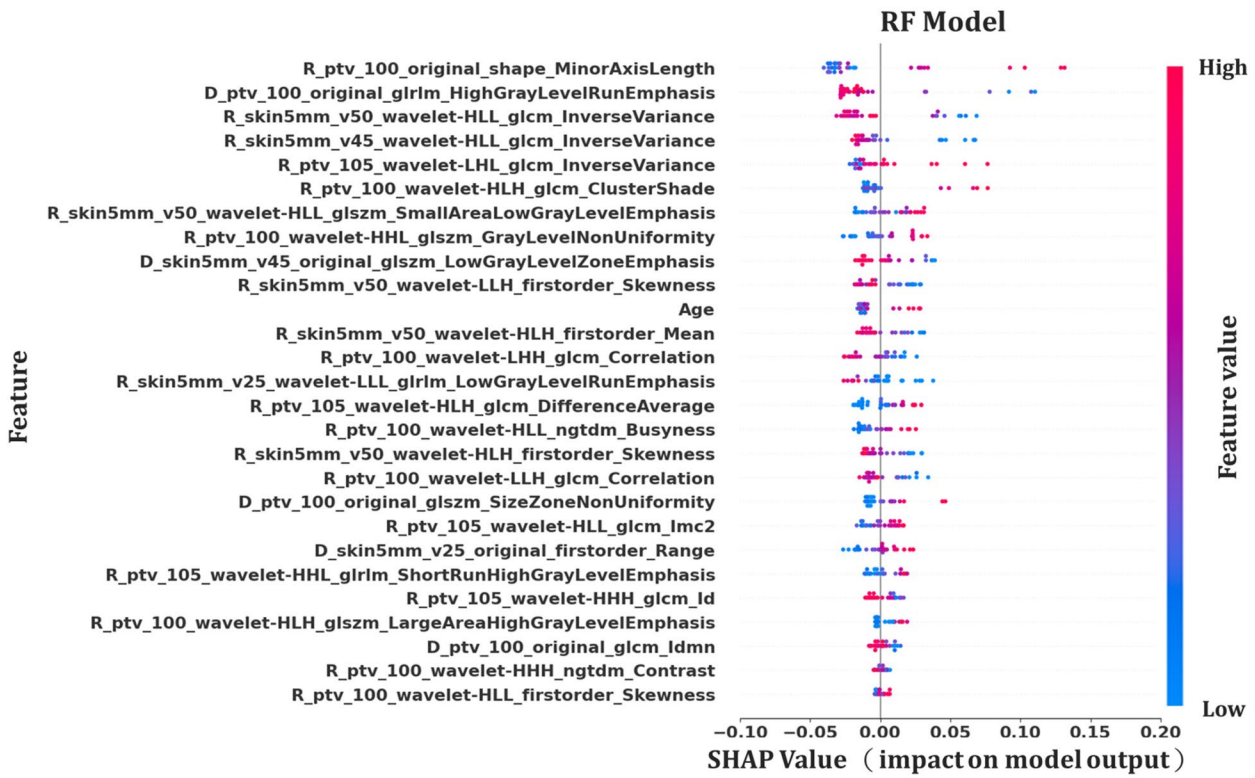

Fig. 6 Bee Swarm Plot of Feature Importance via SHAP Values in the RF Model for Predicting Grade 2^+ RD. Abbreviation: RF, Random Forests; R, Radiomicd; D, Dosiomics; RD, Radiation Dermatitis; SHAP, SHapley Additive exPlanations

(Grade 2^+ RD: 24.74, < Grade 2^+ RD: 23.2), suggesting a lower prevalence of overweight and obese patients, who are typically beyond the standard BMI range.

Our study highlights the correlation between age and the incidence of Grade 2^+ RD, supported by both ANOVA and LASSO regression analysis, aligning with findings from Córdoba et al. [30], which noted increased severe skin toxicity in older women. This suggests that aging may reduce physiological resilience, like blood flow and DNA repair, enhancing susceptibility to severe skin reactions. Conversely, broader research, including studies referenced [7, 27], generally shows minimal correlation between age and RD severity, pointing to potential influences from sample demographics, size, and feature distribution in the analysis, which might introduce inconsistencies in findings.

In analyzing the influence of various features on RD prediction, Figs. 5 and 6 provide crucial insights into the SHAP value comparison between the LR and RF models. The LR model highlights age as a significant factor affecting RD risk, with SHAP values ranging from -0.2 to 0.4, suggesting that older age groups are more likely to develop Grade 2^+ RD. In contrast, the RF model shows a more uniform distribution of feature impacts across all features, with age impact values ranging from -0.05 to 0.05, indicating a more balanced and robust integration of predictors across diverse clinical scenarios. This balanced feature influence enhances the RF model's potential for stable predictions. Moreover, the feature 'R_skin5mm_v50_wavelet-HLL_glcm_InverseVariance' stands out in both models, underscoring the importance of textural uniformity in the skin area receiving 50 Gy, processed through wavelet transformation. This feature's significant impact in both models highlights its crucial role in predicting RD, emphasizing how texture uniformity correlates with radiation response.

Every breast cancer patient undergoing RT is fitted with a custom thermoplastic mold to ensure proper immobilization and repeatability. This setup may lead to an increase in the surface dose of the breast [31, 32]. In previous studies, this aspect was not considered [7]. In response, the current practice adjusts for this by deducting 3 mm for the thermoplastic mold when calculating and planning the ROI for Radiomics and Dosiomics within the TPS, establishing a baseline for the actual skin of the patient.

Furthermore, considering the epidermal, dermal, and subcutaneous layers of the skin [33], and based on findings by Hälg et al. [34] that the vascular distribution in the skin is approximately at an average depth of about 5 mm, this study aims to preserve the vascular tissues of the patient's skin to maintain its functionality. Thus, the ROIs for the skin areas of patients are delineated with a thickness of 5 mm below the actual skin.

In this study, we did not specifically address data imbalance, where 33 patients experienced RD and 69 did not, to maintain the authenticity of the dataset and reflect real clinical scenarios. Using VMAT provides effective dose control, thus naturally resulting in a lower incidence rate of RD. We utilized stratified k-fold cross-validation in our training processes to maintain consistent class ratios, partially mitigating the impact of imbalance. Moreover, we conducted repeated ten-fold cross-validations to ensure model stability and reliability. The RF model, which performs well in handling data imbalances, showed promising results. These approaches helped reduce the potential negative effects of the imbalance on model performance while keeping the dataset representative of the clinical environment.

This study also has some limitations and constraints. Firstly, the relatively small sample size and the overall proportion of toxic endpoints might affect the results of statistical analysis, suggesting that future studies with larger sample sizes are needed to validate these findings. The application of Radiomics and Dosiomics methods in observing the development of RD toxicity in breast cancer patients is still limited. Moreover, the delineation of ROI conducted by different professionals such as physicians and physicists may introduce variability, which was not accounted for in this study.

Future research will focus on integrating our predictive model for RD into clinical workflows, significantly enhancing treatment planning and patient management in the field of radiation oncology. The plan involves embedding the model directly into existing TPS, enabling oncologists to assess RD risk in real-time and adjust treatment parameters based on individual patient risk profiles. This strategy not only allows for personalized treatment adjustments, such as dose fractionation and advanced skin-sparing techniques, especially for high-risk patients, but also supports real-time monitoring during treatment. This facilitates proactive treatment adaptations and improves communication with patients regarding potential side effects. Post-treatment, the model aids in identifying patients who require early dermatological intervention, thus enhancing care outcomes. As treatment outcome data continue to be collected and analyzed, this will further refine the model's accuracy and reliability, making it a valuable tool for enhancing the precision and efficacy of radiation therapy in clinical settings. Additionally, future research will explore how to leverage this model to support broader clinical environments, promoting more personalized and effective patient management.

Conclusion

This investigation employed Radiomics and Dosiomics analyses on treatment planning CT images, utilizing the RF algorithm, to enhance the prediction of Grade 2^+ RD in breast cancer patients. By assessing various RD-related ROIs, the integration of Radiomics and Dosiomics features was found to significantly improve the model's predictive power, achieving an AUC of 0.83, surpassing the predictive capabilities of traditional DVH parameters and clinical features alone. Although challenges persist in measuring skin doses precisely, this study highlights how Radiomics and Dosiomics provide innovative avenues for RD prediction. Notably, Radiomics insights suggest that the uniformity of skin tissue plays a crucial role in RD occurrence, offering valuable guidance for clinicians and medical physicists to optimize patient care during radiation therapy. The findings reinforce the importance of integrating clinical, DVH, Radiomics, and Dosiomics features for robust feature selection, utilizing ANOVA and the LASSO methods, which are closely linked to Grade 2^+ RD. This approach lays the groundwork for personalized radiation treatment planning and underscores the benefits of extracting significant features from extensive radiomic and dosiomic datasets, enhancing precision in clinical applications.

Supplementary Information

The online version contains supplementary material available at https://doi.org/10.1186/s12885-024-12753-1.

Additional file 1: Supplementary Table S1. Detailed Features of the 10 Feature Subsets Identified by LASSO.

Acknowledgements
This study was supported financially, in part, by grants from the National Science and Technology Council (NSTC) of the Executive Yuan of the Republic of China, (111-2221-E-992-016-MY2), and (113-2221-E-992-011-MY2). Part of this study was presented as a thesis in Chinese.

Authors' contributions
Conceptualization: T-F. L., P-J.C., S-A. Y.
Data curation: Y-H. L., Y-W. H., P-Y. Y., C-H. C., C-S. S., C-D. T.
Methodology: P-J. C., S–H. L, Y-H. L., J-C. S., C-L. C.
Project administration: T-F. L., P-J. C., S–H. L., S-A. Y.
Writing ± original draft: T-F. L., C-H. C.
Revised paper: T-F. L., Y-C. H., Y-W. L.
Final paper: T-F. L.
All authors reviewed the manuscript.

Funding
Grants from the National Science and Technology Council (NSTC) of the Executive Yuan of the Republic of China, (111–2221-E-992–016-MY2) and (113–2221-E-992–011-MY2).

Availability of data and materials
The datasets used and analyzed during the current study available from the corresponding author on reasonable request. Because of legal restrictions and ethics, the data in this manuscript are available upon formal request from the corresponding author.

Declarations

Ethics approval and consent to participate
This study, involving human participants, received the necessary approval from the Institutional Review Board (IRB) at Kaohsiung Veterans General Hospital, under the approval number KSVGH23-CT12-09, ensuring compliance with ethical standards and regulatory requirements and the Informed Consent Form was waived.

Consent for publication
Not applicable.

Competing interests
All authors have declared that no competing interests exist.

Author details
[1]Medical Physics and Informatics Laboratory of Electronics Engineering, National Kaohsiung University of Science and Technology, Jiangong RdSanmin Dist., No.415, Kaohsiung 80778, Taiwan, ROC. [2]Graduate Institute of Clinical Medicine, Kaohsiung Medical University, Kaohsiung 807, Taiwan, ROC. [3]Department of Medical Imaging and Radiological Sciences, Kaohsiung Medical University, Kaohsiung 80708, Taiwan, ROC. [4]Department of Radiation Oncology, Kaohsiung Veterans General Hospital, Kaohsiung, Taiwan, ROC. [5]Department of Radiation Oncology, Linkou Chang Gung Memorial Hospitaland, Chang Gung University College of Medicine, Linkou, Taiwan, ROC. [6]Department of Medical Imaging and Radiological Sciences, I-Shou University, Kaohsiung 82445, Taiwan, ROC. [7]Department of Radiation Oncology, E-DA Hospital, Kaohsiung 82445, Taiwan, ROC.

Received: 3 April 2024 Accepted: 2 August 2024
Published online: 06 August 2024

References

1. Zhang Y, Huang Y, Ding S, Yuan X, Shu Y, Liang J, Mao Q, Jiang C, Li J. A dosimetric and radiobiological evaluation of VMAT following mastectomy for patients with left-sided breast cancer. Radiat Oncol. 2021;16:1–11.
2. Ramseier JY, Ferreira MN, Leventhal JS. Dermatologic toxicities associated with radiation therapy in women with breast cancer. Int J Women's Dermatol. 2020;6(5):349–56.
3. Dejonckheere CS, Torres-Crigna A, Layer JP, Layer K, Wiegreffe S, Sarria GR, Scafa D, Koch D, Leitzen C, Köksal MA. Non-invasive physical plasma for preventing radiation dermatitis in breast cancer: a first-in-human feasibility study. Pharmaceutics. 2022;14(9).
4. Harper JL, Franklin LE, Jenrette JM, Aguero EG. Skin toxicity during breast irradiation: pathophysiology and management. South Med J. 2004;97(10):989–94.
5. Reddy J, Lindsay W, Berlind C, Ahern C, Smith B. Applying a machine learning approach to predict acute toxicities during radiation for breast cancer patients. Int J Radiat Oncol Biol Phys. 2018;102(3):S59.
6. Xie Y, Hu T, Chen R, Chang H, Wang Q, Cheng J. Predicting acute radiation dermatitis in breast cancer: a prospective cohort study. BMC Cancer. 2023;23(1):537.
7. Lee T-F, Sung K-C, Chao P-J, Huang Y-J, Lan J-H, Wu H-Y, Chang L, Ting H-M. Relationships among patient characteristics, irradiation treatment planning parameters, and treatment toxicity of acute radiation dermatitis after breast hybrid intensity modulation radiation therapy. PLoS ONE. 2018;13(7).
8. Ranjan R, Partl R, Erhart R, Kurup N, Schnidar H. The mathematics of erythema: development of machine learning models for artificial intelligence assisted measurement and severity scoring of radiation induced dermatitis. Comput Biol Med. 2021;139:104952.
9. Kumar V, Gu Y, Basu S, Berglund A, Eschrich SA, Schabath MB, Forster K, Aerts HJ, Dekker A, Fenstermacher D. Radiomics: the process and the challenges. Magn Reson Imaging. 2012;30(9):1234–48.
10. Van Timmeren JE, Cester D, Tanadini-Lang S, Alkadhi H, Baessler B. Radiomics in medical imaging—"how-to" guide and critical reflection. Insights Imaging. 2020;11(1):91.

11. Krafft SP, Rao A, Stingo F, Briere TM, Court LE, Liao Z, Martel MK. The utility of quantitative CT radiomics features for improved prediction of radiation pneumonitis. Med Phys. 2018;45(11):5317–24.
12. Conti A, Duggento A, Indovina I, Guerrisi M, Toschi N. Radiomics in breast cancer classification and prediction. Semin Cancer Biol. 2021;72:238–50.
13. Liang B, Yan H, Tian Y, Chen X, Yan L, Zhang T, Zhou Z, Wang L, Dai J. Dosiomics: extracting 3D spatial features from dose distribution to predict incidence of radiation pneumonitis. Front Oncol. 2019;9.
14. Placidi L, Gioscio E, Garibaldi C, Rancati T, Fanizzi A, Maestri D, Massafra R, Menghi E, Mirandola A, Reggiori G. A multicentre evaluation of dosiomics features reproducibility, stability and sensitivity. Cancers. 2021;13(15).
15. Chopra N, Dou T, Sharp G, Sajo E, Mak R. A combined radiomics-dosiomics machine learning approach improves prediction of radiation pneumonitis compared to DVH data in lung cancer patients. Int J Radiat Oncol Biol Phys. 2020;108(3).
16. Saadatmand P, Mahdavi SR, Nikoofar A, Jazaeri SZ, Ramandi FL, Esmaili G, Vejdani S. A dosiomics model for prediction of radiation-induced acute skin toxicity in breast cancer patients: machine learning-based study for a closed bore linac. Eur J Med Res. 2024;29(1):282.
17. Wu K, Miu X, Wang H, Li X. A Bayesian optimization tunning integrated multi-stacking classifier framework for the prediction of radiodermatitis from 4D-CT of patients underwent breast cancer radiotherapy. Front Oncol. 2023;13.
18. Feng H, Wang H, Xu L, Ren Y, Ni Q, Yang Z, Ma S, Deng Q, Chen X, Xia B. Prediction of radiation-induced acute skin toxicity in breast cancer patients using data encapsulation screening and dose-gradient-based multi-region radiomics technique: a multicenter study. Front Oncol. 2022;12.
19. Van Griethuysen JJ, Fedorov A, Parmar C, Hosny A, Aucoin N, Narayan V, Beets-Tan RG, Fillion-Robin J-C, Pieper S, Aerts HJ. Computational radiomics system to decode the radiographic phenotype. Can Res. 2017;77(21):e104–7.
20. Parmar A, Katariya R, Patel V. A Review on Random Forest: An Ensemble Classifier. In: Hemanth J, Fernando X, Lafata P, Baig Z, editors. International Conference on Intelligent Data Communication Technologies and Internet of Things (ICICI) 2018. ICICI 2018. Lecture Notes on Data Engineering and Communications Technologies, vol 26. Cham: Springer; 2019. p. 758-763. https://doi.org/10.1007/978-3-030-03146-6_86.
21. Macaulay BO, Aribisala BS, Akande SA, Akinnuwesi BA, Olabanjo OA. Breast cancer risk prediction in African women using random forest classifier. Cancer Treatment and Research Communications. 2021;28.
22. Speiser JL, Miller ME, Tooze J, Ip E. A comparison of random forest variable selection methods for classification prediction modeling. Expert Syst Appl. 2019;134:93–101.
23. Xie Y, Wang Q, Hu T, Chen R, Wang J, Chang H, Cheng J. Risk factors related to acute radiation dermatitis in breast cancer patients after radiotherapy: a systematic review and meta-analysis. Front Oncol. 2021;11:738851.
24. Vicini FA, Sharpe M, Kestin L, Martinez A, Mitchell CK, Wallace MF, Matter R, Wong J. Optimizing breast cancer treatment efficacy with intensity-modulated radiotherapy. Int J Radiat Oncol* Biol* Phys. 2002;54(5):1336–44.
25. Jia H, Li R, Liu Y, Zhan T, Li Y, Zhang J. Preoperative Prediction of Perineural Invasion and Prognosis in Gastric Cancer Based on Machine Learning through a Radiomics-Clinicopathological Nomogram. Cancers. 2024;16(3):614.
26. Zhou J, Lu J, Gao C, Zeng J, Zhou C, Lai X, Cai W, Xu M. Predicting the response to neoadjuvant chemotherapy for breast cancer: wavelet transforming radiomics in MRI. BMC Cancer. 2020;20:1–10.
27. Liu D, Zheng Z, Zhang S, Zhu C, Zhang H, Zhou Y. Analysis of risk factors related to acute radiation dermatitis in breast cancer patients during radiotherapy. J Cancer Res Ther. 2022;18(7):1903–9.
28. Behroozian T, Milton L, Li N, Zhang L, Lou J, Karam I, Wronski M, McKenzie E, Mawdsley G, Razvi Y. Predictive factors associated with radiation dermatitis in breast cancer. Cancer Treat Res Commun. 2021;28:100403.
29. Yamazaki H, Yoshida K, Kobayashi K, Tsubokura T, Kodani N, Aibe N, Ikeno H, Nishimura T. Assessment of radiation dermatitis using objective analysis for patients with breast cancer treated with breast-conserving therapy: influence of body weight. Jpn J Radiol. 2012;30:486–91.
30. Córdoba EE, Lacunza E, Güerci AM. Clinical factors affecting the determination of radiotherapy-induced skin toxicity in breast cancer. Radiat Oncol J. 2021;39(4):315.
31. Lee N, Chuang C, Quivey JM, Phillips TL, Akazawa P, Verhey LJ, Xia P. Skin toxicity due to intensity-modulated radiotherapy for head-and-neck carcinoma. Int J Radiat Oncol* Biol* Phys. 2002;53(3):630–7.
32. Kelly A, Hardcastle N, Metcalfe P, Cutajar D, Quinn A, Foo K, Cardoso M, Barlin S, Rosenfeld A. Surface dosimetry for breast radiotherapy in the presence of immobilization cast material. Phys Med Biol. 2011;56(4):1001.
33. Saibishkumar EP, MacKenzie MA, Severin D, Mihai A, Hanson J, Daly H, Fallone G, Parliament MB, Abdulkarim BS. Skin-sparing radiation using intensity-modulated radiotherapy after conservative surgery in early-stage breast cancer: a planning study. Int J Radiat Oncol* Biol* Phys. 2008;70(2):485–91.
34. Hälg RA, Besserer J, Schneider U. Systematic measurements of whole-body dose distributions for various treatment machines and delivery techniques in radiation therapy. Med Phys. 2012;39(12):7662–76.

Publisher's Note